Evaluation of adhesion characteristics of joint in concrete by tension softening properties

K. Yamada, A. Satoh & S. Ishiyama
Akita Prefectural University, Yurihonjo, Japan

ABSTRACT: This study intends to reveal some clues for improving mechanical properties of joint in concrete. The authors conducted fracture mechanics test of nine types of specimens as the models of vertical construction joint. Along with the investigation on fracture mechanics parameters, SEM analysis was made from the samples on detached and fractured surfaces of specimens. The resulted fracture mechanics parameters and tension softening diagram showed clearer difference of performance in joint than flexural strength does. There are many pores and fragmental layers of $Ca(OH)_2$ observed in smooth part of ligament after the test, which could be the main cause of detaching without fracturing of the surface.

1 INTRODUCTION

1.1 *Construction joint*

Every concrete structure has inevitably construction joint that is a discontinuous plane of concrete produced during construction. The joint in concrete induces many types of deterioration to performances, such as decreased tensile strength that also makes shear strength lower (Hamazaki 2003), a higher possibility of water penetration (Tanaka & Shin 2000) and a higher tendency of carbonation through the joint than monolithic concrete with no joint (Yamamoto 2001). Also horizontal joint suffers dry out that changes the pore structure, eventually making the durability performance lower (Yuasa 1998).

The construction joint is also a good example of researching adhesion performance of repair in concrete structure, because the interfacial adhesion is the most critical issue for both of construction joint and repaired surface. There are surging needs for improving interfacial adhesion of concrete (Sakami 2006) as repair and retrofitting of existing concrete structure is a major market of construction industry in developed countries (Sakai 2006).

1.2 *Previous studies*

Many previous studies revealed that additional placing of concrete should be well advanced before hardening of previously placed one, if discontinuity of concrete should be avoided (Yamamoto 2001; Sugata 2003). After hardening, tensile strength between two bodies (a previously placed body and an additionally placed one) decreases depending on many conditions, such as time after the previous one was placed, roughness of the surface where additional one is placed, direction and thickness of concrete layer downward which is related to an amount of bleeding water (Yamamoto 2001; Hamazaki 2003), and so on.

It was common that the adhesion strength of joint was evaluated with bending strength through bending test (Yamamoto 2001; Hamazaki 2003), and there was few study which evaluated tension-softening properties of joint.

Kurihara et al. (1996) investigated 5 types of concrete prism specimens with the results that fracture energy calculated by tension softening diagram (TSD) denotes clear difference in adhesion performance of joint in the specimen. Other than this study, there is no research that employs TSD for an evaluation of adhesion performance.

1.3 *Purpose of the research*

Previous studies do not tell the cause of the decrease of adhesive performance through joint. There have been no studies observing the joint surface with a scanning electron microscope (SEM). Also there is no research discussing the difference of TSD characteristics with varied types of joints; such as cast surface with a delay of 24 hours, or 48 hours, with a mortar layer and with a permanent form made of fiber reinforced cement composites (FRCC).

There is a difference of conditions between horizontal and vertical joint. It is well known that the horizontal joint surface of concrete suffers dry-out and bleeding, which is more complicated than verti-

cal joint surface. Vertical joint surface scarcely suffers such complex combination of condition for concrete, which eventually makes the researching focus on adhesion performance sharp.

Then the authors employed specimens with a vertical joint at the center of them for evaluation of adhesion performance with various types of joint in concrete, and discuss the cause of the decrease from the results of TSD and SEM observation.

2 EXPERIMENT

2.1 *Specimens*

Table 1 and Figure 1 show the attribute and illustration of specimens, and Table 2 the mix proportion in which following materials were used. Cement is ordinary Portland cement. Gravel is crushed stone with the size under 20 mm. Sand is natural pit sand. FRCC board is made of PVA (polyvinyl alcohol) fiber and cement, produced through Hatcheck machine before pre-curing at 50 degree, whose thickness is 6 mm and tensile strength is 12.8 MPa. Joint sheet is made of plastic with many cones on the surface and ordinarily used for vertical joint to give enhanced shear strength (Civil Eng. Res. C. 2002). (See Figure 2).

Table 3 shows the mechanical properties of concrete and mortar, in which the strengths were measured with cylinder type specimens (diameter is 100 mm for concrete and 50 mm for mortar). Other than those specimens, each specimen for fracture toughness test was a prism with a section of 100 mm by 100 and a length of 400 mm. At center of the specimen, a half-depth (50 mm) notch was provided prior to fracture toughness test.

2.2 *Tension softening diagram*

Standard curing in water was applied for 28 days from the cast of the latter concrete. After that, fracture toughness test was executed with observing JCI's standards (Izumi 2004). The only test method that differs from the standard is that the authors provided counter weights at both ends of the specimen to cancel the weight of the specimen. The load was applied at the center of the span and at a speed of 0.06 mm/min with measuring load, deflection and crack mouth opening displacement (CMOD). The loading speed was controlled with a feed-back system to be exactly the same at anytime.

Inverse analysis was adapted to the resulted load-deflection curve to calculate TSD with observing JCI's standards (Izumi 2004). The finite element (FEM) model used in the analysis has 389 elements in half of the specimen and 41 nodes in ligament.

Table 1. Attribute of specimens.

Specimen	Attribute of specimens
R-1	Reference with no joint
D-1	Separated with a piece of dried FRCC board
Dr-1	Separated with a piece of wet FRCC board
F-1	Cast after 24 hours on the surface (slightly roughened with wire brush)
F-2	Cast after 24 hours on the surface (strongly roughened with wire brush)
Fs-1	Cast after 48 hours on the surface whose form was painted steel
Fs-2	Cast after 48 hours on the surface of F-2 specimen
I-1	Cast after 24 hours on the surface whose form was joint sheet
J-1	Cast immediately after on the surface of mortar attached after 24 hours on previously cast concrete

Table 2. Mix proportion of concrete and mortar.

Mixture	Weight of materials				Super Plasticizer
	Water	Cement	Sand	Gravel	
	kg/m^3	kg/m^3	kg/m^3	kg/m^3	kg/m^3
Concrete*	177	344	739	1010	1.72
Mortar	209	523	1569	-	-

* W/C=51.4%, s/a=43%, Air=3%, Slump=16.4cm.

Table 3. Mechanical properties of concrete and mortar.

Mixture	Density	Compressive strength	Tensile strength
	g/cm^3	MPa	MPa
Concrete*	2.31	42.70	3.83
Mortar*	2.20	41.45	3.74

* Cure= 28 days of standard curing in water.

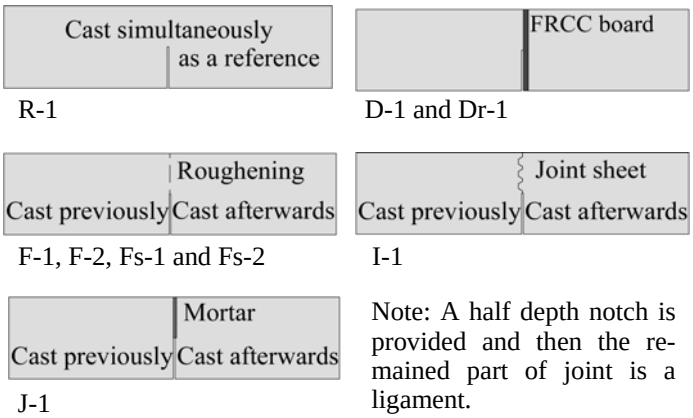

Figure 1. Detail of specimens.

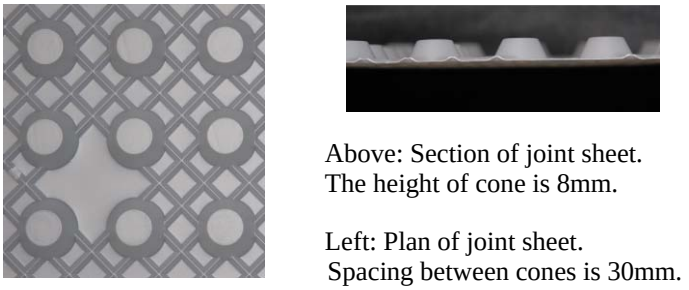

Above: Section of joint sheet. The height of cone is 8mm.

Left: Plan of joint sheet. Spacing between cones is 30mm.

Figure 2. Detail of joint sheet.

3 RESULTS

3.1 *Fracture mechanics parameters*

Table 4 shows the resulted fracture mechanics parameters, in which F_b is flexural strength, F_t is tension softening initial stress, G_F is fracture energy, K_{1c} is stress intensity factor calculated with equation (1) and G_c is energy release rate calculated with equation (2). The values for R-1 are similar to the previous studies (Ohgishi 1988, Kitsutaka 1997).

$$K_{1C} = \frac{PS}{BW^{\frac{3}{2}}}\left\{2.898\left(\frac{a}{W}\right)^{\frac{1}{2}} - 4.613\left(\frac{a}{W}\right)^{\frac{3}{2}} + 21.8\left(\frac{a}{W}\right)^{\frac{5}{2}} - 37.7\left(\frac{a}{W}\right)^{\frac{7}{2}} + 38.74\left(\frac{a}{W}\right)^{\frac{9}{2}}\right\} \quad (1)$$

$$G_C = \frac{K_{1C}{}^2}{E} \quad (2)$$

There are 2 groups recognized in Table 4 except for R-1. One group is F-2, Fs-2, I-1 and J-1, which has large values of F_b and F_t. Other group is D-1, Dr-1, F-1 and Fs-1, which has smaller values than group 1. Though F_b and F_t are almost equal within group1 or group2, fracture mechanics parameters are different ranging from double to triple or moreover. This result is the same as the one from a research by Kurihara (1996).

3.2 *Tension softening diagram*

Figure 3A, 3B and 3C show TSDs. Figure 3A tells that the major difference between R-1 and other two is the closure stress between 0.01 mm and 0.05 mm. It is suggested that this range of closure stress is the major cause of difference for fracture energy. Figure 3B tells that wet surface of the layer of FRCC is essential for improving adhesion performance. Figure 3C tells that the joint with the different roughening produces the different TSD.

Table 4. Resulted fracture mechanics parameters.

Name	F_b	F_t	G_F	K_{1C}	G_c
	MPa	MPa	N/m	MN/m$^{3/2}$	N/m
R-1	6.58	6.82	91.1	0.693	17.73
D-1	1.87	2.50	5.6	0.196	1.31
Dr-1	2.06	2.30	6.2	0.216	1.73
F-1	1.56	1.66	3.1	0.160	0.87
F-2	4.29	4.70	23.6	0.454	7.61
Fs-1	2.87	3.33	17.5	0.299	3.31
Fs-2	3.92	3.75	39.8	0.413	5.82
I-1	4.22	5.40	35.1	0.383	5.01
J-1	4.22	5.10	36.6	0.439	7.04

F_b: Flexural strength, F_t: Tension softening initial stress
G_F: Fracture energy, K_{1C}: Stress intensity factor
G_c: Energy release rate

The ratio of G_F divided by that of weakest joint reaches moreover 10 (F-1 vs. Fs-2) in Table 4, indicating the adequate roughening is very essential for the enhanced performance of the joint. In the roughened joints, the order of G_F is F-1 < Fs1 < F-2 < Fs2, meaning cast after 48 hours has good results.

FRCC permanent form did not have good results in this test, but it can be pointed out that pre-wetting of the form should be the requisite for improved adhesion because D-1 < Dr-1 in G_F.

The interesting finding is that the better the G_F becomes, the larger the critical width when closure stress becomes zero (Figure 3A - 3C).

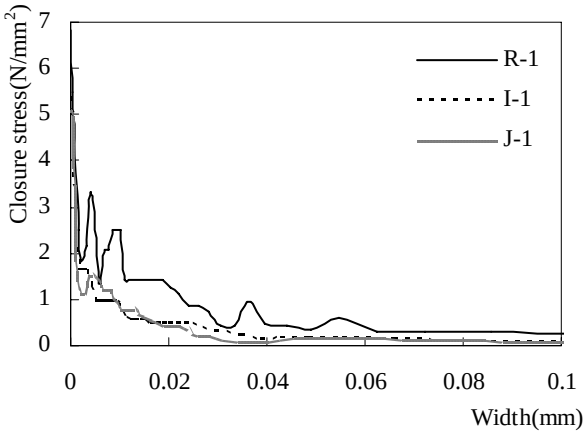

Figure 3A. TSDs for R-1, I-1 and J-1.

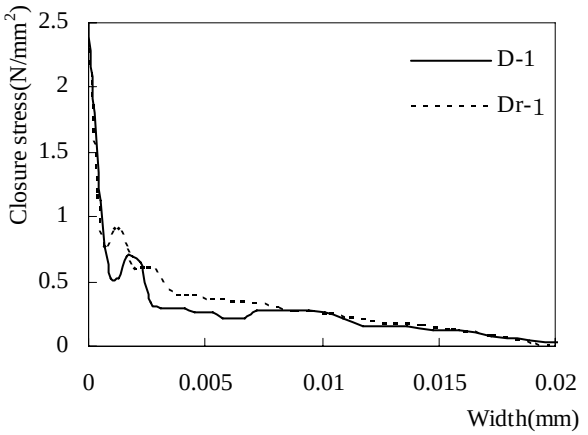

Figure 3B. TSDs for D-1 and Dr-1.

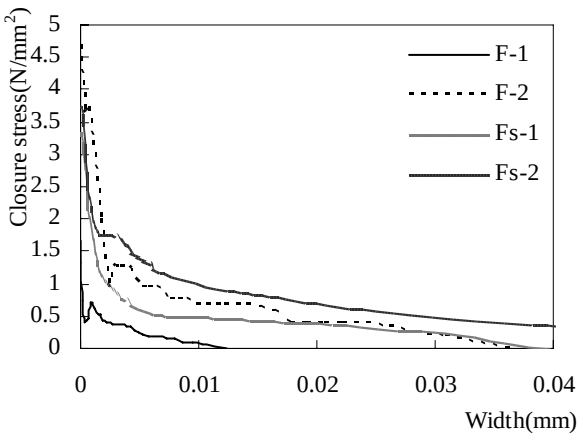

Figure 3C. TSDs for F-1, F-2, Fs-1 and Fs-2.

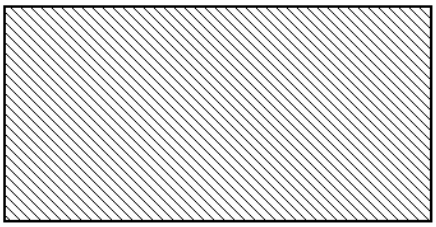
R-1

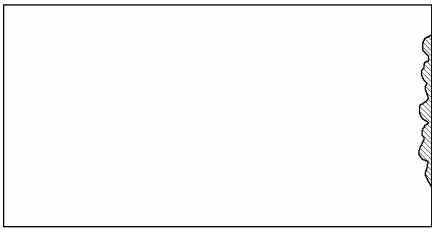
D-1


Dr-1


F-1

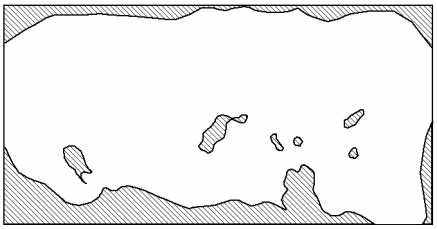
F-2

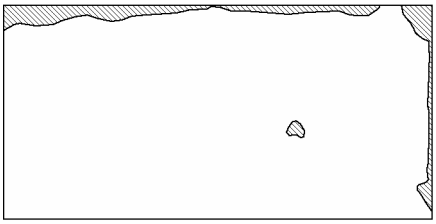
Fs-1

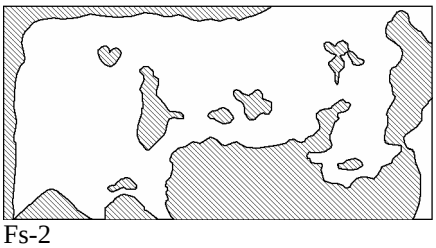
Fs-2

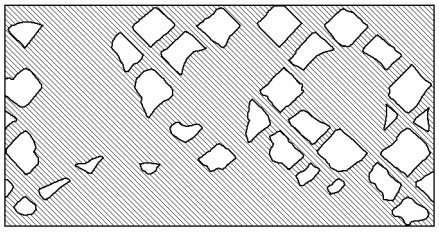
I-1

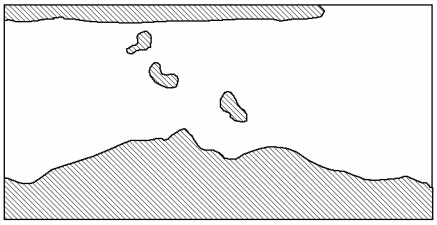
J-1

Note: Dashed area indicates fractured rough part while blank area indicates detached smooth part.

Figure 4. Map of fractured part and detached part.

3.3 *Observation of fracture surface*

There are two types of fracture surfaces at the ligament of the specimen after fracture toughness test. One is a fractured part, the other is a detached part. The authors made careful observation on the surface, and the smooth surface was determined as a detached part and rough surface as a fractured part.

Figure 4 depicts the map of them. The dashed area indicates fractured part while blank area detached smooth part in ligament.

4 DISCUSSIONS

4.1 *F_b and fractured area*

If the detached part in ligament of the specimen does not contribute to the flexural strength, F_b should be proportional to the moment of inertia calculated only with the fractured part. At the beginning of the first crack when stress of the tensile edge becomes F_b, the neutral axis can be assumed to be the center of ligament. Then the moment of inertia calculated within the tensile fractured part would be proportional to the F_b.

These assumptions are described in following equations (3) and (4), and depicted in Figure 5. In Figure 5, x-axis represents J_r / J_A and y-axis F_b.

$$M_{cr} = \int \sigma y dA = \frac{\sigma}{y} J_r = \sigma_0 J_r \tag{3}$$

$$F_b = \frac{M_{cr}}{J_A} \frac{h}{2} = \sigma_0 \frac{h}{2} \frac{J_r}{J_A} = k \frac{J_r}{J_A} \tag{4}$$

Where M_{cr} = bending moment at cracking, σ_0 = stress at unit height from the neutral axis, k= constant, J_r =moment of inertia for only fractured tensile part and J_A = moment of inertia for all tensile part.

The location of the symbols above the solid line indicates that the smooth part that was not considered as effective should be considered as effective for adhesion strength. On the contrary, the location of symbols below the solid line tells vice versa, and also the possibility of the weaker strength for the fractured part than that of reference.

There are two groups in this graph. One group gathers near y-axis, which tells detached part has some contribution to F_b. The other group has relatively high F_b (4 MPa) and they locates near the solid line that connect origin and R-1, telling that these assumptions can be correct for them.

4.2 *G_F and fractured area*

If total area in ligament is available for G_F, it can be calculated with equation (5). If fractured part distributes uniformly within the section, G_F only by the fractured part of specimen (G_{F-part}) should be proportional to the fraction of fractured part to total area in ligament (ϕ), resulting in equation (6).

$$G_F = \frac{E(w) + E'(w)}{A_{lig}} \quad (5)$$

$$G_{F-part} = G_F \phi \quad (6)$$

Where $E(w)$ = consumed energy in load-deflection curve until crack width is w, $E'(w)$ = differentiated $E(w)$ with respect to w, A_{lig} = total area of ligament, ϕ = fraction of fractured area to total area, k= some constant and G_{F-part} = G_F of specimen that has a smaller width than a full width.

Equation (5) derives from equation (7) that is well known equation usually employed for calculation of closure stress with modified J-integral method (Uchida 1991).

$$\sigma(w) = \frac{wE''(w) + 2E'(w)}{A_{lig}} \quad (7)$$

Where $\sigma(w)$ = closure stress and $E''(w)$ = differentiated $E'(w)$ with respect to w.

In Figure 6, x-axis represents ϕ and y-axis represents G_F. Almost all symbols (except for Fs-1 and I-1) locate near the solid line that connects origin and R-1, telling that these assumptions can be correct for them.

The distance of the same symbol from the solid line is different between Figure 5 and 6, which suggests that the governing cause of F_b and G_F is different. It means that even detached part contributes to F_b (even smooth surface could bear stress by chemical bond), whereas visibly rough surface is necessary for consuming energy like G_F.

The reason for the poor performance in both F_b and G_F produced from fractured part in the case of I-1 may be the weakness of the adhesion strength, which may derive from the produced $Ca(OH)_2$ by plastic joint sheet.

4.3 *SEM observation in detached part*

The authors cut a sample of 1 cm square from the surface of each specimen. After platinum spattering on it, SEM observation was done. Figure 7A – 7F show typical observations of a surface of concrete that was cast afterwards on the surface of previously cast one.

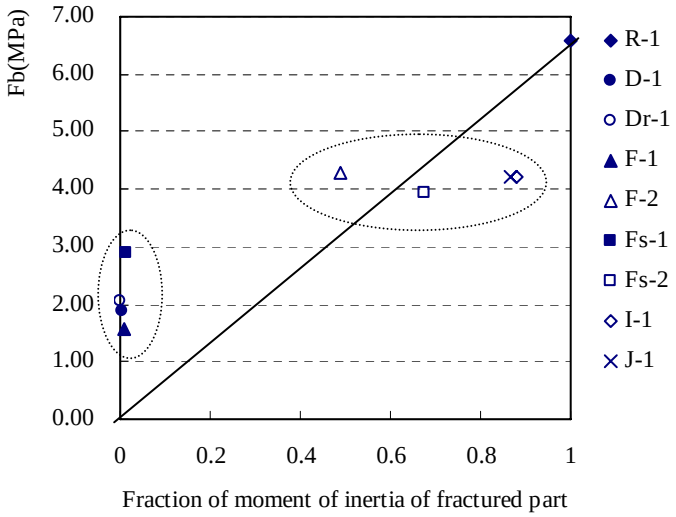

Figure 5. Relationship between flexural strength and fractured area.

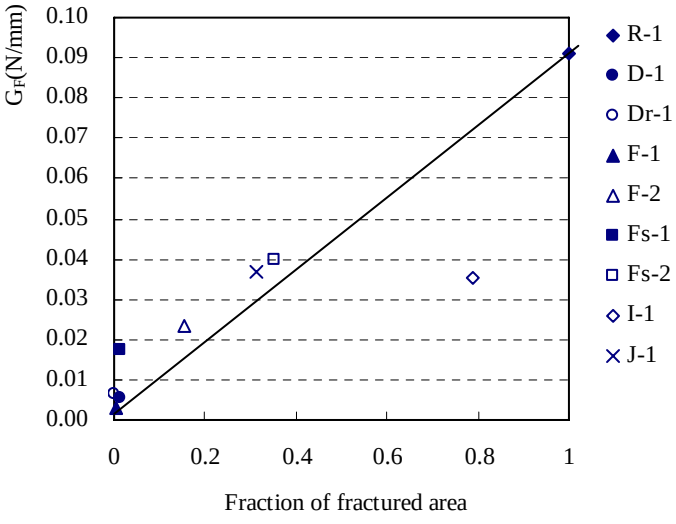

Figure 6. Relationship between fracture energy and fracture area.

Many pores are seen on the surface that contacted to FRCC board in Figure 7A. The air is considered to come from FRCC board, because the surface of the board is rough enough to entrap large pores on the surface. Smooth surface in Figure 7B is $Ca(OH)_2$ because element analysis told Ca= 73.0% and Si= 22.5%. This was produced during the hydration on the surface of form and remained after wire brushing of the surface. Rough surface is the usual observation in fractured part like Figure 7C in R-1 specimen. On the other hand, smooth surface in Figure 7D is aggregate because element analysis told that Na= 13.5%, Al= 18.2%, Si= 61.3% and Ca= 4.2%.

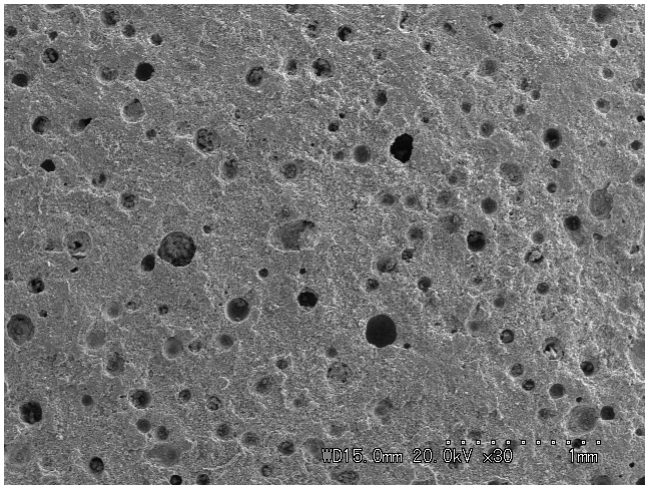

Figure 7A. SEM photo from detached part in D-1 (x30).

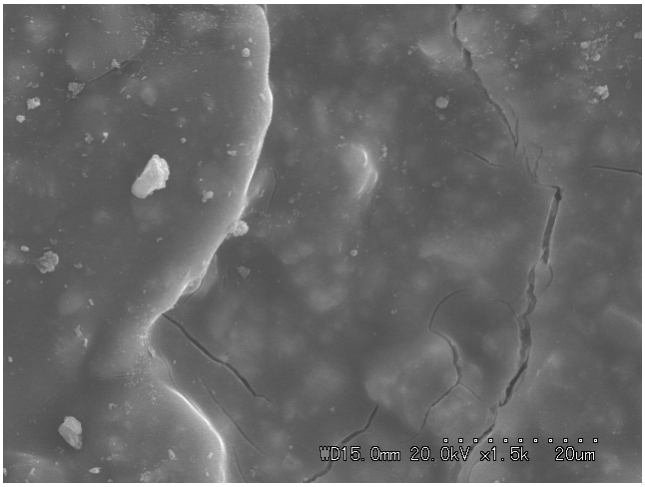

Figure 7B. SEM photo from detached part in Fs-2 (x1500).

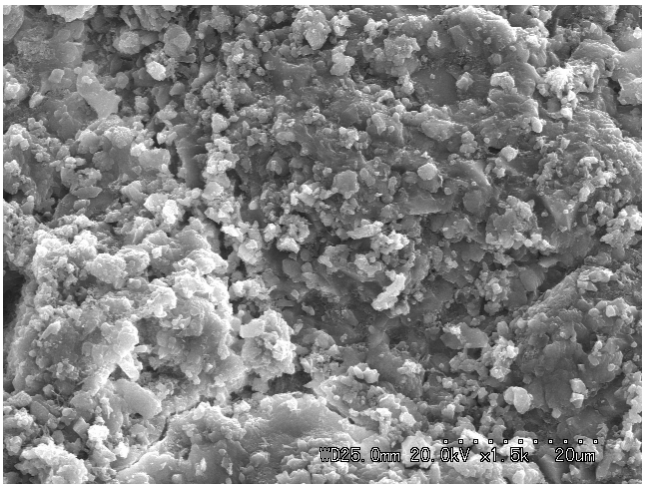

Figure 7C. SEM photo from fractured part in R-1 (x1500).

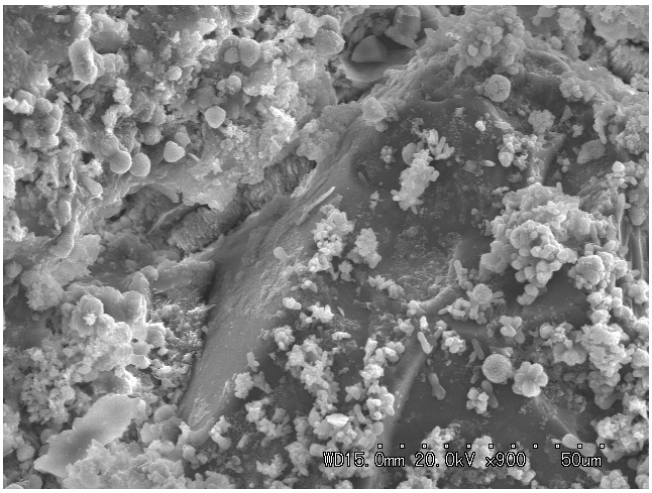

Figure 7D. SEM photo from fractured part in Fs-1 (x900).

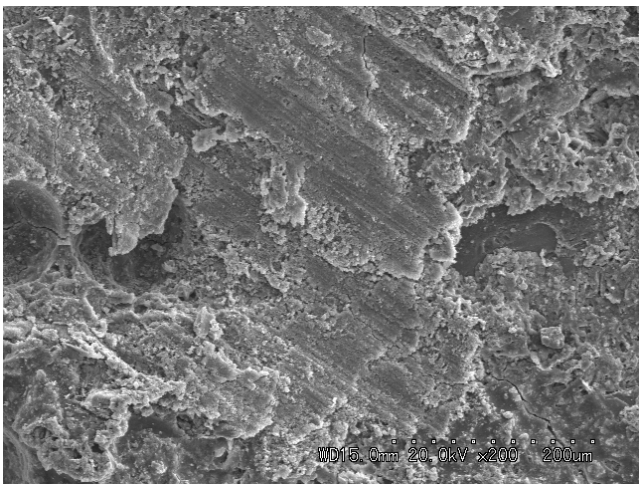

Figure 7E. SEM photo from detached part in F-2 (x200).

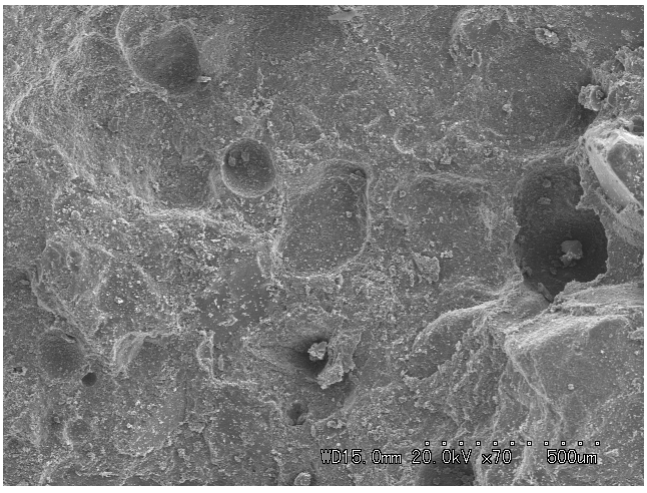

Figure 7F. SEM photo from fractured part in J-1 (x70).

From Figure 7D, it is suggested that transient layer (Uchikawa 1993, Kobayashi 1998) on the aggregate near the surface of joint may have fractured and the aggregate appeared.

The surface that have scratches in Figure 7E is made of $Ca(OH)_2$ because element analysis told Ca= 78.1% and Si= 21.9%. Thus $Ca(OH)_2$ remains on the surface of previously cast concrete after roughening by wire brush.

Figure 7F shows fractured surface of mortar layer on J-1 specimen. There are some holes where grains of sand torn off and some grains of sand remained on the surface.

In summary, there are many pores and a layer of $Ca(OH)_2$ observed in detached part, which could be the main cause of detaching. On the other hand, rough surface of CSH gel and transient layer around aggregate are observed in fractured part. There are grains of sand and holes where grains of sand torn off along with gravels (that are avoided for SEM observation).

5 CONCLUSIONS

Fracture mechanics parameters and tension softening diagram of nine types of specimens for vertical construction joint were examined along with SEM analysis from the samples on detached and fractured surfaces.

The findings are as follows.

[1] Even though flexural strengths at ligament of nine specimens are not substantially different from each other, fracture energies of them are substantially different from each other. The authors point out that the key to improve the structural performance of joint should be the enhancement of fracture energy.

[2] Smooth surface of detached part that appears on specimen after fracture toughness test can contribute to flexural strength, whereas it cannot contribute to fracture energy. This suggests that the mechanism of determining the strength and the fracture energy is different with each other.

[3] There are many pores and layer of $Ca(OH)_2$ observed in detached part, which could be the main cause of detaching. Then, some of the keys to enhance the performance of joint are thoroughly removing a layer of $Ca(OH)_2$, or to find mix proportions or conditions with which $Ca(OH)_2$ does not produce in joint.

REFERENCES

Civil Eng. Res. C. (eds) 2002. *Evidence report on inspection of construction technology No. 0123* Tokyo: Civil Eng. Res. C.

Hamazaki, J. 2003. Study on evaluation and prevention method of discontinuous joint of concrete. *Annual report of Building Research Institute of Japan* 2001: 71-72.

Izumi, I. (eds) 2004. *Test method for fracture energy of plain concrete (Draft) in JCI standards* Tokyo: JCI.

Kitsutaka, Y. & Oh-oka, T. 1997. Influence of short cut fiber on fracture parameters of high strength mortar matrix. *J. Struct. Constr. Eng. by AIJ* 497: 1-8.

Kobayashi, K. et al. 1996. Characters of interfacial zone of cement paste with additives around aggregate. *J. Mat. Sci. Japan* 45(9): 1001-1007.

Kurihara, T. et al. 1996. Evaluation of adhesive performance of construction joint in concrete by tension softening diagram. *Proc. annual meeting of JCI* 18(2): 461-466.

Ogawa, A. et al. 2005. PVA-fiber reinforced high performance cement board, *Proc. Int'l workshop on high performance fiber reinforced cementitious composites in structural applications (Hawaii)* Task Gr. C: 1-8.

Ohgishi, S. & Ono, H. 1988. Influence of testing factors on fracture toughness, G1c and fracture energy, G_F of plain and fiber reinforced concrete. *Concrete technology* 26(2): 103-118.

Sakai, E. 2006. Methods of cross sectional restoration. *Cement and concrete* 713: 39-44

Sakami, S. (eds) 2006. *Check list for construction joint in RC structures* Tokyo: Gihodo.

Sugata, N. et al. 2003. Improvement of union of concrete by placing process. *Cement science and Concrete technology* 57: 186-192.

Tanaka, K. & Shin, Y. 2000. Permeability and pore structure of placing joint of cement mortar in casting. *J. Struct. Constr. Eng. by AIJ* 529: 7-12.

Uchida, Y. et al. 1991. Determination of tension softening diagrams of concrete by means of bending tests. *Journal of JSCE in V-1* 426: 203-212.

Uchikawa, H. et al. 1993. Estimation of the thickness of transition zone in hardened mortar and concrete, and investigation of the relationship between their thickness and strength development. *Concrete research and technology* 4(2): 1-8.

Yamamoto, Y. (eds) 2001. *Counter plans and problems for cold joint in concrete structure: Concrete library 103 by JSCE* Tokyo: Maruzen.

Yuasa, N. et al. 1998. Inhomogeneous distribution of the moisture content and porosity from the surface layer to internal parts. *J. Struct. Constr. Eng. by AIJ* 509: 9-16.